



CHORUS

This is the accepted manuscript made available via CHORUS. The article has been published as:

Anionic and Hidden Hydrogen in ZnO

Mao-Hua Du and Koushik Biswas

Phys. Rev. Lett. **106**, 115502 — Published 16 March 2011

DOI: [10.1103/PhysRevLett.106.115502](https://doi.org/10.1103/PhysRevLett.106.115502)

Anionic and “Hidden” Hydrogen in ZnO

Mao-Hua Du and Koushik Biswas

Materials Science and Technology Division and Center for Radiation Detection

Materials and Systems, Oak Ridge National Laboratory, Oak Ridge, Tennessee 37831,

USA.

First-principles calculations are performed to study energetics and kinetics of hydrogen in ZnO, in particular, the H^- anion and the H_2 molecule on the interstitial site and in the oxygen vacancy. We show that the H_2 molecule kinetically trapped in the oxygen vacancy, rather than interstitial H_2 , can explain a variety of experimental observations on “hidden” hydrogen in ZnO. The accumulation of shallow donors, especially the substitutional H, near ZnO surface is important to the formation of “hidden” hydrogen in ZnO bulk and can also lead to persistent photoconductivity.

PACS: 61.72.S-, 61.72.jd, 61.72.Cc, 71.55.-i

ZnO is a promising wide-gap semiconductor for blue/UV optoelectronics¹ and is also a fast scintillator that may be used for radiation detection.² Hydrogen in ZnO has been extensively studied in the last ten years^{3, 4, 5, 6, 7, 8, 9, 10, 11, 12, 13, 14, 15} because unintentionally doped H is usually found in ZnO, including many commercial ZnO samples.⁶ Interstitial and substitutional H have been shown by first-principles calculations to be shallow donors (i.e., H_i^+ and H_O^+), which contribute to the *n*-type conductivity in ZnO.^{3, 12} Subsequent experiments confirmed that hydrogen incorporation increases the electron carrier density in ZnO.⁶ The O-H vibrational frequencies have also been observed by IR spectroscopy.^{4, 5, 8, 9}

Annealing experiments have been performed to understand the thermodynamics and kinetics of H in ZnO. High temperature (750 °C-1000 °C) annealing of ZnO in the H₂ environment incorporates a large amount of H_i and H_O ($10^{17} - 10^{18} \text{ cm}^{-3}$) in ZnO.^{6, 13, 14} Subsequent quenching and annealing at lower temperatures removes atomic hydrogen from ZnO. H_i can be annealed out of ZnO at 150 °C while H_O is eliminated between 500 °C to 700 °C.⁶ It appears that a “hidden” hydrogen reservoir exists in ZnO and can release H_i when the temperature is > 400 °C.⁶ The “hidden” hydrogen species are invisible by the IR spectroscopy. The interstitial H₂ molecule (H_{2,int}) was suggested to be a candidate for the “hidden” hydrogen.⁶ Recently, H₂ molecules have indeed been identified by a Raman study when ZnO is annealed without external hydrogen at 550 °C following annealing at 1000 °C in an H₂ environment.¹⁴

Despite this progress, we find that the H behavior is nontrivial and far from being understood. In particular, if assuming the “hidden” hydrogen is H_{2,int}, the H behavior cannot be reconciled with basic thermodynamic principles. First of all, the basic question

that needs to be answered is whether H_i^+ or $H_{2,int}$ is the more stable hydrogen species in ZnO. Obviously, this depends on the hydrogen chemical potential and Fermi level. The higher the H chemical potential, the more likely the diatomic species like H_2 would be more stable. Also, since H_i^+ is a donor while $H_{2,int}$ is neutral, the $[H_i^+]/[H_{2,int}]$ ratio should increase with decreasing Fermi level. High-temperature annealing under H_2 environment provides a condition that is close to the thermal equilibrium for H in ZnO. Under this condition, H_i^+ is found to be abundant while no H_2 is found,¹⁴ which suggests that H_i^+ is more stable than H_2 . However, with subsequent annealing at lower temperatures without external H (lower H chemical potential), H_i^+ disappears (which results in lower Fermi level) while H_2 appears.¹⁴ It is thus puzzling that a lower H chemical potential and a lower Fermi level promote the formation of $H_{2,int}$ at the expense of H_i^+ . These conflicting results for hydrogen in ZnO warrant a re-examination of the hydrogen energetics and kinetics in ZnO.

Besides the above puzzling experimental results, there are also unanswered fundamental questions on H chemistry in ZnO. H in ZnO has been predicted by theory and confirmed experimentally to be a shallow donor, rather than an amphoteric impurity,^{3,6} meaning that the H (+/-) level is above the conduction band minimum (CBM). However, the H_i^- structure has never been identified. The H_i^- ion discussed in the literature, i.e. bond-center (BC) or anti-bonding (AB) H_i^- coordinated with one oxygen atom, is actually an H_i^+ with two free electrons.³ Thus, from theoretical point of view, the proof of H_i as a shallow donor in ZnO is not complete until we find both H_i^+ and H_i^- structures and calculate the (+/-) transition level. The knowledge of chemistry of

anionic hydrogen is important to the understanding of hydrogen chemistry in ZnO and in semiconducting and ionic materials in general.

We have carried out a comprehensive study of the interactions of atomic hydrogen (including both H_i^+ and H_i^- ions) and H_2 molecules with the ZnO lattice and the low-energy oxygen vacancy (V_O). We show that the (+/-) transition level for H_i is located at 0.34 eV above CBM. We also suggest that the H_2 local vibrational modes (LVMS) observed by Raman spectroscopy may originate from an H_2 molecule trapped in an oxygen vacancy ($V_O^{2+}-H_2$) rather than from $H_{2,int}$. As a result of the H_O^+ accumulation near the surface, $V_O^{2+}-H_2$ should exist in the interior of the ZnO sample where the Fermi level is lower and also the persistent photoconductivity may occur due to the surface band bending.

Our calculations are based on the plane-wave projector augmented wave method¹⁶ with Heyd-Scuseria-Ernzerhof (HSE) hybrid functional.^{17, 18} unless otherwise noted, as implemented in the vasp code.^{19, 20} The screening parameter of the non-local Fock exchange is set at 0.2 \AA^{-1} .¹⁸ We use 37.5% of the non-local Fock exchange in the HSE functional to produce a band gap of 3.47 eV, which is in good agreement with the experimental value. The cutoff energy for the plane-wave basis is 400 eV. All the calculations were performed using 96-atom supercells. A $2 \times 2 \times 2$ grid was used for the k-point sampling of the Brillouin zone. All the atoms were relaxed to minimize the Feynman-Hellmann forces to below 0.05 eV/\AA . The methods for calculating formation energies and transition energy levels can be found in Ref. 21.

We will begin by discussing the interaction of H^- with the ZnO lattice and the oxygen vacancy. We find that H_i^- prefers to be located in the hollow hexagonal channel,

binding with three Zn atoms, as shown in Fig. 1(a), rather than on BC or AB sites as investigated in Ref. 3. Multi-coordination is often seen for ionic bonding, which is governed by Coulomb attraction and electron shell repulsion.²² (H_i^+ is an exception as it has no electron shell and thus favors a single bond.) H_i^- in ZnO induces a fully occupied deep gap level (H 1s level) at $E_v + 1.66$ eV. However, H_i^- is only metastable as shown in Fig. 2. The (+/-) transition level for H_i is 0.34 eV above the CBM, explaining why H_i is a shallow donor in ZnO.

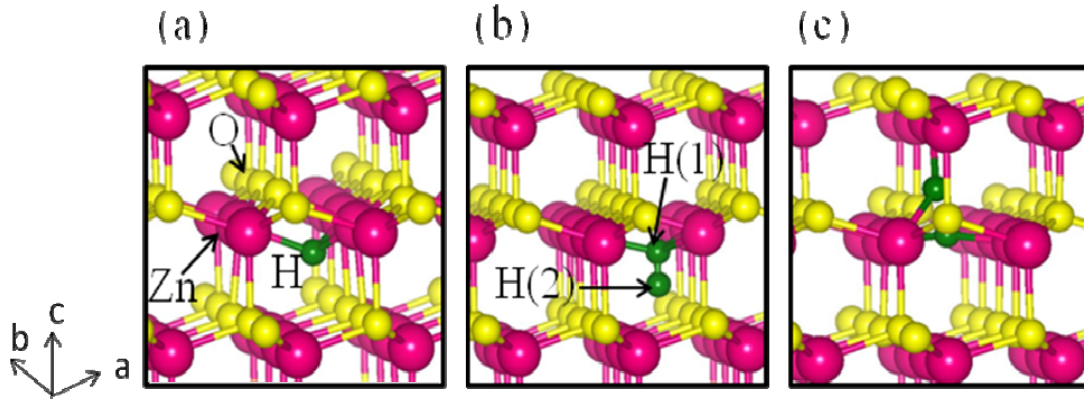


FIGURE 1. (Color online) Structures of (a) interstitial H^- ion (H_i^-), (2) interstitial H_2 ($H_{2,int}$), and (3) two H^- ions in an oxygen vacancy ($V_O^{2+} - 2H^-$).

We have shown previously that H^- can bind with anion vacancies in II-VI semiconductors.²² H^- may be located on or off-center in the anion vacancy, depending on the size of the anion vacancy relative to the ionic radius of H^- . In the case of ZnO, H^- occupies the center of V_O^{2+} , effectively forming a substitutional H_O^+ . Here, we find that a V_O can further trap a second H^- to form $V_O^{2+} - 2H^-$, with overall charge state to be neutral. In $V_O^{2+} - 2H^-$, each H^- binds with two Zn atoms as shown in Fig. 1(c). Based on the calculated formation energy of 1.63 eV (assuming O-poor and H-rich limits), the

concentration of $V_{\text{O}}^{2+} - 2\text{H}^-$ in ZnO should range from 10^{14} to 10^{16} cm^{-3} if ZnO is hydrogenated at 750-1000 °C. One should also be aware that $V_{\text{O}}^{2+} - 2\text{H}^-$ may be sensitive to light excitation since it induces a fully occupied deep level at $E_{\text{v}} + 0.77$ eV and it is known that H^- in the anion vacancy of alkali halides is a color center (*U* center).^{23, 24, 25} Removing one or two electrons from the deep gap level of $V_{\text{O}}^{2+} - 2\text{H}^-$ will change the distance between the two H atoms from 2.10 to 1.07 or 0.75 Å. With two electrons removed, the H-induced level will be cleared from the band gap and the two H^- ions become an H_2 molecule. The occupied deep level by $V_{\text{O}}^{2+} - 2\text{H}^-$ can be viewed as the filled anti-bonding orbital of an H_2 molecule.

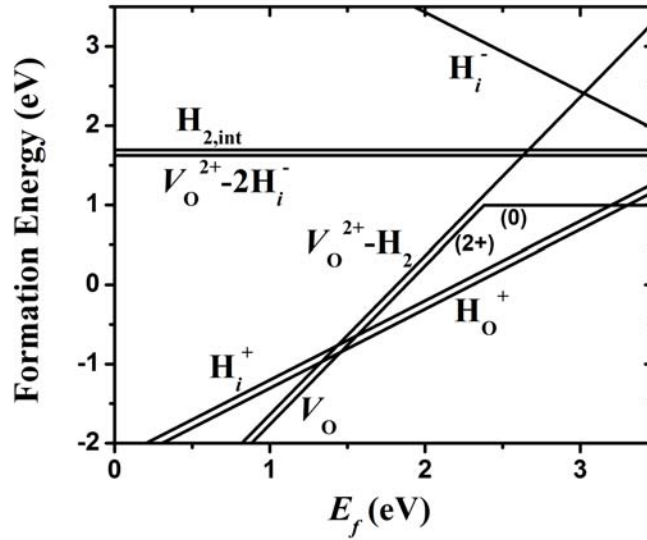


FIGURE 2. Formation energies of hydrogen and oxygen vacancy related defects in ZnO. The slope of the energy lines indicates the charge state of the defect, as selectively shown. The point, at which the slope changes, is the transition energy level.

The calculated Zn-H stretching modes for $V_{\text{O}}^{2+} - 2\text{H}^-$ are 1875 ($\perp c$ axis) and 1692 ($\parallel c$ axis) cm^{-1} , respectively. These LVMs have not been observed. However, based on

the calculated formation energy and defect concentration, these LVMs may be observable by IR spectroscopy provided that ZnO is hydrogenated at high temperature (>1000 °C) and that the light excitation of the H^- -induced deep level is avoided.

Our calculations show that H_i^+ is more stable than $H_{2,int}$ in the entire range of accessible Fermi energy (see Fig. 2). This is consistent with the experimental observation of H_i^+ but not H_2 after hydrogenation at high temperature (>1000 °C),¹⁴ which provides a condition close to the thermal equilibrium for H in ZnO. The results shown in Fig. 2 assume an H-rich condition. One should note that reducing the H chemical potential will increase the formation energy of $H_{2,int}$ faster than that of H_i^+ . Surprisingly, the LVMs of H_2 is observed by Raman spectroscopy while H_i^+ is annealed out at lower temperature (550 °C) without external H (lower H chemical potential). These results suggest that the H_2 molecules that are observed by Raman spectroscopy may not be $H_{2,int}$.

The interstitial H_2 is aligned along the c axis in the hollow hexagonal channel in ZnO.^{3,10} As may be seen from Figs. 1(a) and (b), one of the H atoms in $H_{2,int}$ occupies a position close to the H_i^- site. The Zn-H bond lengths are 1.85 and 1.98 Å for H_i^- and $H_{2,int}$, respectively. It is, therefore, conceivable that $H_{2,int}$ is slightly polarized with the H(1) in Fig. 1(b) slightly negatively charged whereas the H(2) is slightly positively charged. The calculated LVMs for $H_{2,int}$ and $D_{2,int}$ are 4460 and 3154 cm^{-1} , respectively. When both H and D are present, the LVMs for HD_{int} are either 3875 or 3861 cm^{-1} , depending on whether D occupies the H(1) or H(2) site. The splitting of the H-D stretching modes by 14 cm^{-1} is not insignificant, reflecting the fact that the H(1) and H(2) sites are not equivalent as a result of Zn-H(1) bonding. However, the polarization of $H_{2,int}$

is small and it should therefore still be Raman active. Raman spectroscopy with resolution $<5 \text{ cm}^{-1}$ did not find such H-D mode splitting.¹⁴ This further casts doubt on whether the observed H_2 LVMs indeed result from $\text{H}_{2,\text{int}}$.

Here we propose that the “hidden” hydrogen in ZnO is the H_2 molecule trapped in the oxygen vacancy ($V_{\text{O}}^{2+}-\text{H}_2$). The H_2 in V_{O}^{2+} is surrounded by four Zn atoms that are located at the vertices of an approximate tetrahedron. As a result, the H_2 in V_{O}^{2+} has nearly no polarization, in contrast to $\text{H}_{2,\text{int}}$, and is nearly a free rotator as also suggested experimentally.¹⁴ The calculated H_2 , D_2 , and HD LVMs are in excellent agreement with experimental results, as shown in Table I. In particular, the H-D LVM splitting is negligible, consistent with the experiments.

Table I. Local vibrational frequencies (LVMs) of calculated and measured H_2 , D_2 , and HD in the interstitial site and oxygen vacancy of ZnO. The LVMs of the free H_2 molecule are also shown. The units are in cm^{-1} .

	$\text{H}_{2,\text{int}}$	$\text{D}_{2,\text{int}}$	HD_{int}	$V_{\text{O}}^{2+}-\text{H}_2$	$V_{\text{O}}^{2+}-\text{D}_2$	$V_{\text{O}}^{2+}-\text{HD}$	Free H_2
Theory	4460	3154	3875 3861	4277	3025	3705 3703	4448
Exp.				4145 [†]	2985 [†]	3628 [†]	4395 [‡]

[†] Ref. 14; [‡] Ref. 26

ZnO is typically *n*-type with the Fermi level near CBM. Under this condition, $\text{H}_{2,\text{int}}$ should be more stable than $V_{\text{O}}^{2+}-\text{H}_2$ as shown in Fig. 2. However, the interior of the ZnO sample can be much more insulating, favoring the formation of $V_{\text{O}}^{2+}-\text{H}_2$. The “hidden” hydrogen was suggested to form in the temperature range of 150 - 450 °C, in which H_i^+ is annealed out while H_O^+ remains.⁶ The H_2 LVMs were observed by Raman spectroscopy in a much larger-sized ZnO sample annealed at 550 °C for 30 minutes.¹⁴

The annealing was sufficient to eliminate all H_i^+ but the annealing time was too short to anneal out all H_O^+ ,²⁷ which has a much higher diffusion barrier than H_i^+ .^{11, 12} In both cases, the majority of the H donor, i.e., H_i^+ , is eliminated.²⁸ As a result, the carrier density is substantially lowered. The remaining dominant donor, H_O^+ , is heavily concentrated near the ZnO surface because the oxygen vacancies are mostly created near the surface during high-temperature annealing.^{13, 15} The H_O^+ penetration depth is shown to be 5-6 μm when ZnO undergoes H annealing at 750 $^\circ\text{C}$.¹⁵ Zn interstitials (Zn_i), which are highly mobile native donors,^{29, 30, 31} are also likely to accumulate near the surface because the extra Zn_i resulted from quenching of ZnO from high temperature (as was done in Ref. 6 and 14) may tend to phase-separate to the surface. As a result, the surface band bending occurs, creating a depletion layer extending from the surface to the interior of the ZnO sample. The interior of the ZnO sample should have much lower carrier density and Fermi level. As shown in Fig. 2, the lower Fermi level promotes the formation of V_O^{2+} and hence $V_O^{2+} - H_2$. Meanwhile, the non-equilibrium factor also plays a role in ionizing V_O^0 . The oxygen vacancy in ZnO is a color center in ambient environment,³² indicating strong light absorption by V_O^0 leading to the formation of V_O^{2+} . The photo-ionization of V_O^0 has been suggested to contribute strongly to the n -type conductivity in ZnO.³³ Therefore, the combination of low carrier density in bulk and the high light absorption at V_O^0 may lead to the formation of $V_O^{2+} - H_2$ in bulk ZnO. Indeed, it was found that Raman spectroscopy of H_2 LVMS is sensitive to the excitation spot in the ZnO sample,²⁷ and that H_2 and H_O^+ in ZnO anti-correlate,¹⁴ which means that H_2 is not distributed near the

surface. Our V_{O}^{2+} -H₂ model predicts that H₂ should be located in the bulk near the boundary of the surface depletion region. However, there is no mechanism to justify the anti-correlation between H_{2,int} and H_O⁺.

During the high temperature hydrogenation, the carrier density is very high in bulk ZnO due to the existence of large amount of fast-diffusing H_i⁺ (Ref. 7 and 11). Such environment favors V_{O}^0 over V_{O}^{2+} and consequently suppresses the formation of H₂@ V_{O}^{2+} . This explains why H₂ LVMs are not detected in high-temperature hydrogenated ZnO.¹⁴

V_{O}^{2+} -H₂ is a metastable species. It is unstable against the following reaction, V_{O}^{2+} -H₂ → H_i⁺+H_O⁺, which lowers the energy by 0.87 eV. H_i⁺ is unstable when T > 150 °C. Therefore, the observation of H₂ LVMs at 550 °C should be due to the kinetic trapping of H₂ by V_{O}^{2+} . The trapping energy is calculated to be 1.57 eV. In comparison, the diffusion barrier of H_{2,int} is calculated to be 0.9 eV along the *c* axis and 0.6 eV on the *a-b* plane using Perdew-Burke-Ernzerhof exchange correlation functionals.³⁴ We believe that the experimental condition, in which H₂ LVMs were detected by Raman spectroscopy,¹⁴ is a non-equilibrium condition. Both H_O⁺ and H₂ should be in the process of out diffusion at 550 °C. We suspect that the Raman signal of H₂ LVMs will not survive after prolonged annealing. The weak Raman signal of H₂ LVMs and the sensitivity of the Raman signal to the excitation spot¹⁴ suggest low density and inhomogeneous distribution of H₂ in ZnO. The detection of V_{O}^{2+} -H₂ requires an optimal annealing temperature and annealing time. If the annealing temperature is too high, no H₂ can survive. If it is too low, there would be too many H_O⁺ in ZnO, which not only competes with H₂ for O vacancy sites but

also supplies electron carriers that suppress the formation of V_{O}^{2+} in favor of V_{O}^0 . Another prerequisite for V_{O}^{2+} -H₂ formation in ZnO is high-temperature hydrogenation, which creates oxygen vacancies. According to our best knowledge, there has not been a report on “hidden” hydrogen or on the detection of H₂ LVMs in ZnO treated by low-temperature H plasma, which can also introduce H into ZnO but does not create large quantity of oxygen vacancies.

Finally, we note that the good thermal stability of H₀⁺ allows it to exist in ZnO (including many commercial samples)^{9, 13} unless ZnO is annealed at high temperature (>500 °C) for sufficiently long time. This should result in surface band bending, which further has the effect of rapid separation of photo-generated electrons and holes, leading to persistent photoconductivity.

We thank E. V. Lavrov and S. Lany for stimulating discussions. This work was supported by the U.S. DOE Office of Nonproliferation Research and Development NA22.

-
- ¹ K. Klingshirn, *phys. stat. sol. (b)* **244**, 3027 (2007).
- ² W. W. Moses, *Nucl. Instr. Meth. Phys. Res. A* **487**, 123 (2002).
- ³ C. G. Van de Walle, *Phys. Rev. Lett.* **85**, 1012 (2000).
- ⁴ M. D. McCluskey, S. J. Jokela, K. K. Zhuravlev, P. J. Simpson, K. G. Lynn, *Appl. Phys. Lett.* **81**, 3807 (2002).
- ⁵ E. V. Lavrov, J. Weber, F. Börrnert, C. G. Van de Walle, and R. Helbig, *Phys. Rev. B* **66**, 165205 (2002).
- ⁶ G. A. Shi, M. Saboktakin, M. Stavola, S. J. Pearton, *Appl. Phys. Lett.* **85**, 5601 (2004).
- ⁷ K. Ip. M. E. Overberg, Y. W. Heo, D. P. Norton, S. J. Pearton, C. E. Stutz, B. Luo, F. Ren, D. C. Look, and J. M. Zavada, *Appl. Phys. Lett.* **82**, 385 (2003).
- ⁸ S. J. Jokela and M. D. McCluskey, *Phys. Rev. B* **72**, 113201 (2005).
- ⁹ G. A. Shi, M. Stavola, S. J. Pearton, M. Thieme, E. V. Lavrov, and J. Weber, *Phys. Rev. B* **72**, 195211 (2005).
- ¹⁰ M. G. Wardle, J. P. Goss, and P. R. Briddon, *Phys. Rev. B* **72**, 155108 (2005).
- ¹¹ M. G. Wardle, J. P. Goss, and P. R. Briddon, *Phys. Rev. Lett.* **96**, 205504 (2006).
- ¹² A. Janotti and C. G. Van De Walle, *Nature Materials* **6**, 44 (2007).
- ¹³ E. V. Lavrov, F. Herklotz, and J. Weber, *Phys. Rev. B* **79**, 165210 (2009).
- ¹⁴ E. V. Lavrov, F. Herklotz, and J. Weber, *Phys. Rev. Lett.* **102**, 185502 (2009).
- ¹⁵ F. Herklotz, E. V. Lavrov, and J. Weber, *Physica B* **404**, 4349 (2009).
- ¹⁶ P. E. Blöchl, *Phys. Rev. B* **50**, 17953 (1994).
- ¹⁷ J. Heyd, G. E. Scuseria, and M. Ernzerhof, *J. Chem. Phys.* **118**, 8207 (2003).

-
- ¹⁸ J. Heyd, G. E. Scuseria, and M. Ernzerhof, *J. Chem. Phys.* **125**, 224106 (2006).
- ¹⁹ G. Kresse and J. Furthmüller, *Phys. Rev. B* **54**, 11169 (1996).
- ²⁰ G. Kresse and D. Joubert, *Phys. Rev. B* **59**, 1758 (1999).
- ²¹ M.-H. Du, H. Takenaka, and D. J. Singh, *Phys. Rev. B* **77**, 094122 (2008).
- ²² M.-H. Du and D. J. Singh, *Phys. Rev. B* **79**, 205201 (2009).
- ²³ W. Martienssen, *Z. Physik* **131**, 488 (1952).
- ²⁴ S. S. Mitra and Y. Brada, *Phys. Rev.* **145**, 626 (1966).
- ²⁵ G. A. Tanton, R. A. Shatas, R. S. Singh, and S. S. Mitra, *J. Chem. Phys.* **52**, 538 (1969).
- ²⁶ K. P. Huber and G. Herzberg, *Molecular Spectra and Molecular Structure. IV: Constants of Diatomic Molecules*, Van Nostrand Reinhold, New York (1972).
- ²⁷ E. V. Lavrov, private communication.
- ²⁸ The experimental results suggest higher $[H_i^+]$ than $[H_O^+]$ (Ref. 9). On the other hand, Fig. 2 shows that the calculated formation energies of H_i^+ is slightly higher than that of H_O^+ , meaning lower $[H_i^+]$ than $[H_O^+]$. The calculations assumed thermal equilibrium and the extreme O poor growth condition, which may not reflect the real experimental condition.
- ²⁹ Y. V. Gorelkinskii, and G. D. Watkins, *Phys. Rev. B* **69**, 115212 (2004).
- ³⁰ C. Coskun, D. C. Look, G. C. Farlow, and J. R. Sizelove, *Semicond. Sci. Technol.* **19**, 752 (2004).
- ³¹ A. Janotti and C. G. Van de Walle, *Phys. Rev. B* **76**, 165202 (2007).

³² L. E. Halliburton, N. C. Giles, N. Y. Garces, M. Guo, C. Xu, L. Bai, and L. A. Boatner, *Appl. Phys. Lett.* **87**, 172108 (2005).

³³ S. Lany and A. Zunger, *Phys. Rev. Lett.* **98**, 045501 (2007).

³⁴ J. P. Perdew, K. Burke, and M. Ernzerhof, *Phys. Rev. Lett.* **77**, 3865 (1996).